

Positive carbon isotope excursions: global correlation and genesis in the Middle–Upper Ordovician in the northern Tarim Basin, Northwest China

Cun-Ge Liu^{1,2} · Li-Xin Qi² · Yong-Li Liu² · Ming-Xia Luo² · Xiao-Ming Shao² · Peng Luo² · Zhi-Li Zhang³

Received: 27 April 2015 / Published online: 23 April 2016
© The Author(s) 2016. This article is published with open access at Springerlink.com

Abstract Stable carbon isotope ratio ($\delta^{13}\text{C}_{\text{carb}}$) analysis has been widely applied to the study of the inter-continental or global marine carbonate correlation. Large-scale Cambrian–Ordovician carbonate platforms were developed in the Tarim Basin. But research on fluctuation characteristics and global correlation of $\delta^{13}\text{C}_{\text{carb}}$ is still weak. Based on conodont biostratigraphy and whole-rock $\delta^{13}\text{C}_{\text{carb}}$ data in the Tahe oil–gas field of the northern Tarim Basin, the global correlation and genesis of positive carbon isotope excursions in the Darriwilian–Early Katian was examined. Three positive excursions were identified in the Tahe oil–gas field including the middle Darriwilian carbon isotope excursion (MDICE), the Guttenberg carbon isotope excursion (GICE), and a positive excursion within the *Pygodus anserinus* conodont zone which is named the Early Sandbian carbon isotope excursion (ESICE) in this paper. Furthermore, these positive excursions had no direct relation with sea level fluctuations. MDICE and GICE could be globally correlated. The Middle–Upper Ordovician Saergan Formation source rocks of the Kalpin outcrops were in accordance with the geological time of MDICE and ESICE. GICE had close relationship with the source rock of the Lianglitag Formation in the basin.

Massive organic carbon burial was an important factor controlling the genesis of these positive excursions.

Keywords Tarim Basin · Tahe oil–gas field · Middle–Upper Ordovician · Carbon isotope · Darriwilian · Sandbian · Katian source rock

1 Introduction

The stable carbon isotope ratio in dissolved inorganic carbon ($\delta^{13}\text{C}_{\text{carb}}$) reflects the initial isotope composition in the original seawater (Saltzman 2005; Ainsaar et al. 2010; Munnecke et al. 2011). Diagenesis to a certain degree cannot change the isotope fluctuation trend (Saltzman 2005). Paleoceanographic environment change results in the death of many organisms and the burial of ^{12}C in them, which can enrich the ^{13}C in the sea water and hence increase the $\delta^{13}\text{C}_{\text{carb}}$ values of carbonate rocks (Sial et al. 2013). $\delta^{13}\text{C}_{\text{carb}}$ fluctuation is taken as an indicator of environmental change (Ainsaar et al. 2010). During the past decades, $\delta^{13}\text{C}_{\text{carb}}$ had been widely used in studies of regional or global correlation on marine carbonate strata and paleoceanographic environment (Zhang et al. 2010a; Ainsaar et al. 2010; Fan et al. 2011).

The Ordovician is a special period in geological history in which some significant events happened, such as the Great Ordovician Biodiversification Event, Late Ordovician glaciation and one mass extinction (Trotter et al. 2008; Monnecke et al. 2010; Zhang et al. 2010b; Thompson et al. 2012). At present, three short-lived $\delta^{13}\text{C}_{\text{carb}}$ -positive excursions have been globally identified in the Ordovician (Zhang et al. 2010a; Sial et al. 2013), including the middle Darriwilian carbon isotope excursion (MDICE), Early Katian Guttenberg carbon isotope excursion (GICE), and

✉ Cun-Ge Liu
liucunge@163.com

¹ State Key Laboratory of Oil and Gas Reservoir Geology and Exploitation, Chengdu University of Technology, Chengdu 610059, Sichuan, China

² Northwest Oilfield Company, China Petroleum & Chemical Corporation, Urumqi 830011, Xinjiang, China

³ Institute of Petroleum Exploration and Development, China Petroleum & Chemical Corporation, Beijing 100083, China

the Hirnantian carbon isotope excursion (HICE). It is generally considered that the MDICE and GICE are closely related to the burial of abundant organic matter (Rosenau et al. 2012; Pancost et al. 2013; Sial et al. 2013), and Hirnantian glaciation and biotic extinction events are closely related to HICE (Zhang et al. 2010a; Monnecke et al. 2011).

In 1990s, the $\delta^{13}\text{C}_{\text{carb}}$ negative excursions were used to investigate Cambrian–Ordovician sea level changes in the Kalpin outcrops of the Tarim Basin (Wang and Yang 1994). In addition, Wang (2000) employed $\delta^{13}\text{C}_{\text{carb}}$ -positive excursions as the proof of marine source rock developing in the Middle–Upper Ordovician. In recent years, some scholars have been engaged in the study of carbon isotope stratigraphy at Cambrian–Ordovician outcrops in the Kalpin and Bachu regions (Jing et al. 2008; Hu et al. 2010; Wang et al. 2011; Zhao 2015). Zhang et al. (2014) discussed $\delta^{13}\text{C}_{\text{carb}}$ curve features of the Ordovician using analyses of cores and cuttings from the Bachu and Tazhong uplifts (Fig. 1a) and concluded the existence of two $\delta^{13}\text{C}_{\text{carb}}$ -positive excursions in the Dapingian–Darriwilian and Sandbian–Early Katian.

In this paper, whole-rock carbon and oxygen isotope and conodont analyses were undertaken on the cores from two wells of the Tahe oil–gas field, Akekule uplift (Fig. 1b). On the basis of conodont biostratigraphy, the identified $\delta^{13}\text{C}_{\text{carb}}$ -positive excursions were compared with those found in the Tarim Basin and other regions of the world. The genetic relationships of $\delta^{13}\text{C}_{\text{carb}}$ -positive excursions with sea level fluctuation, source rocks, and kerogen thermal evolution were also investigated.

2 Geological setting

The Tarim plate had broken from Gondwana and moved as an independent plate during Cambrian. The plate moved from north to south to the equator in the Middle Ordovician (Wang et al. 2013a; Torsvik and Cocks 2013) and was close to the northwestern margin of Gondwana. Large carbonate platforms had been developed in the western part of the plate during the Cambrian–Middle Ordovician (Wu et al. 2012). The Tarim plate had moved northward in the Late Ordovician, when three small carbonate platforms formed in the Tabei Uplift, Bachu–Tazhong Uplift, and Kalpin area in the Early Katian (Hu et al. 2010; Liu et al. 2012).

The Tahe oil–gas field is located in the Akekule uplift of the northern Tarim Basin (Fig. 1b). According to the lithology and well logging features, the Lower–Middle Ordovician can be divided into Penglaiba, Yingshan, and Yijianfang Formations, and the Upper Ordovician is composed of the Qiaerbak, Lianglitag, and Sangtamu

Formations. The Lower–Middle Ordovician exhibits platform facies, and the margins of the platforms were located in the eastern region of what is now the Tahe oilfield (Fig. 1b).

The lithology of the Penglaiba Formation is gray dolomite and sandwiched limy dolomite, characterized by restricted platform facies. The Yingshan Formation which deposited on open platforms is composed of yellowish-gray limestone and thin-bedded calcarenite with dolomitization intensified in the lower part. The Yijianfang Formation consists of yellowish-gray calcarenites sandwiched with thin-bedded limestones and deposited in a shoal environment. Deng et al. (2007) considered the Yijianfang Formation as a Highstand System Tract (HST). The conodont fauna from the Penglaiba Formation to the Yijianfang Formation has North American Midcontinent species (Zhao et al. 2006), characterized by warm water, low abundance, and slow evolution of species. It is difficult to carry out stratigraphic correlation using conodonts in these strata (Wang et al. 2007).

The Qiaerbak Formation consists of drowned platform deposits. The lithology of the lower part is grayish-green muddy limestone, which belongs to a transgressive system tract (TST). The lithology of the upper part is red-brown nodular argillaceous limestone, which belongs to an HST (Wu et al. 2012). The conodont fauna of this formation is of the North Atlantic type, which is characterized by cold water, high abundance, and more species (Zhao et al. 2006). The *Nemagraptus gracilis* graptolite zone is taken as the boundary of the Middle–Upper Ordovician globally, but this boundary is higher than that of the *P. anserinus* conodont zone at the bottom of Upper Ordovician (Chen and Wang 2003; Wang et al. 2013b). Therefore, grayish-green muddy limestones under the finger peak of gamma ray curves should partly belong to the Middle Ordovician (Fig. 2). Red-brown nodular argillaceous limestone of the upper part of the Qiaerbak Formation is a marker bed in the Tabei Uplift (Fig. 1a). The geological time of the Qiaerbak Formation is equal to that of the Kanling Formation in the Kalpin outcrop (Zhao et al. 2006). The lithology and color of the marker bed can be easily distinguished.

The Lianglitag Formation consists of limestones, calcarenites, and muddy limestone and was deposited in carbonate ramp environments containing both TST and HST sequences (Liu et al. 2012; Wu et al. 2012). The ramp margin was distributed circularly (Fig. 1b) with the thickness of strata thinning eastward and southward. The thickness of the Lianglitag Formation of the Tahe oil–gas field is between 10 and 120 m, and that of the Kalpin outcrop is 163.7 m (Hu et al. 2010). The thickness of the Lianglitag Formation of the Tazhong Uplift is between 200 and 800 m (Liu et al. 2012), and is larger than that of the Tahe oil–gas field and Kalpin region. The conodonts are

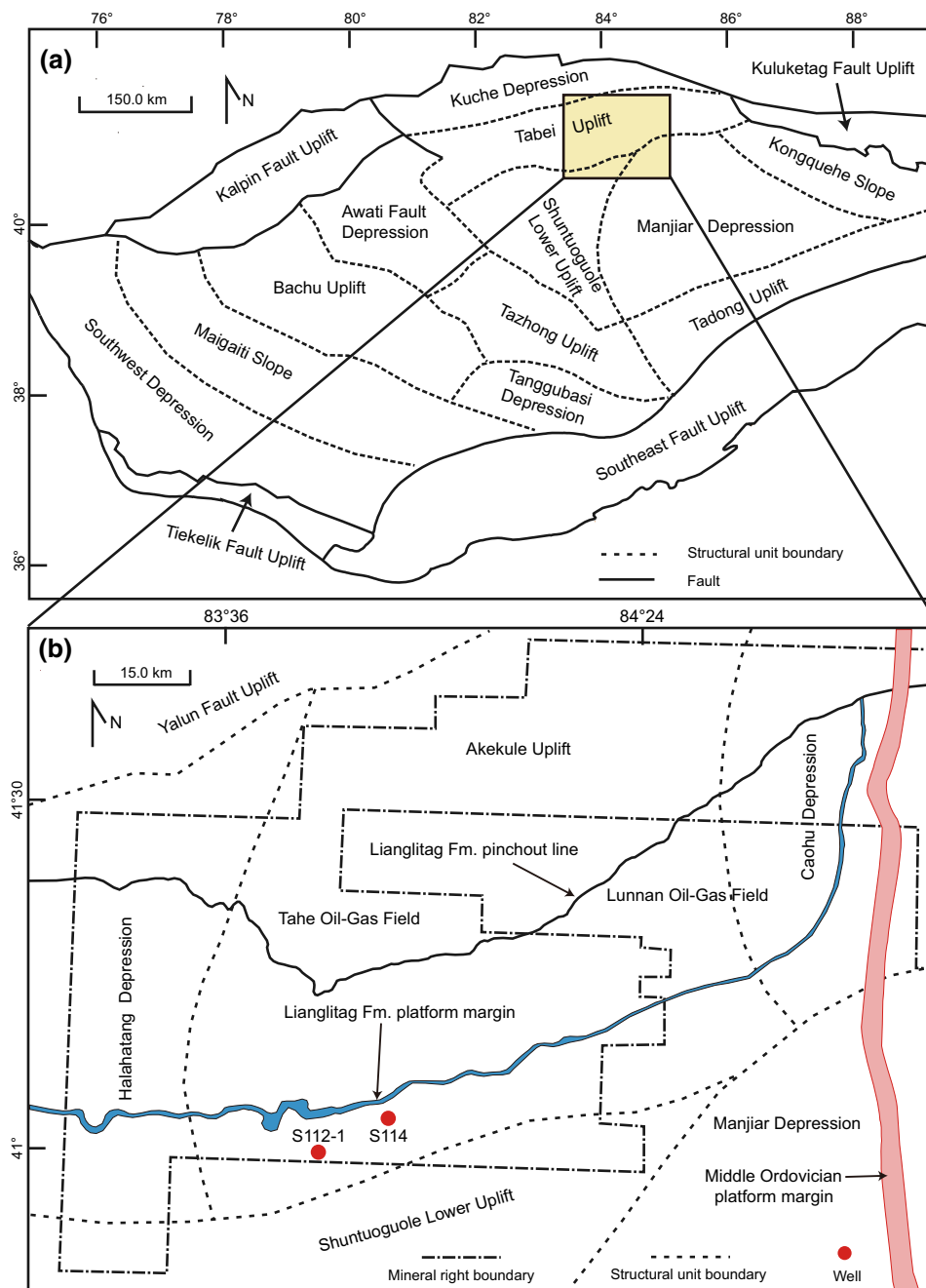


Fig. 1 Location map of the Tahe oil–gas field in the Tarim Basin. **a** The division map of structural units of the Tarim Basin. **b** Geological map of the Middle–Upper Ordovician in the Tahe oil–gas field

from the North American Midcontinent fauna. Typical conodont zones were lacking on the top of the Qiaerbak Formation and Lianglitag Formation. A *Belodina compressa* conodont zone generally developed from the upper Qiaerbak Formation to the Lianglitag Formation (Zhao et al. 2006).

The Sangtamu Formation is deep-water shelf deposits. The lower part is composed of grayish-black mudstone, and the upper part consisted of grayish-black mudstone and

thin-bedded argillaceous limestone. The *Yaoxianognathus neimengguensis* conodont zone can be found at the top of the Lianglitag Formation and developed mostly in the Sangtamu Formation (Zhao et al. 2006).

A short-term deposition hiatus occurred at the end of both the Yijianfang Formation and Lianglitag Formation (Liu et al. 2010; Chen et al. 2013) in the Akekule Uplift. The exposed area of the Yijianfang Formation appears mainly in the eastern and northern region. The

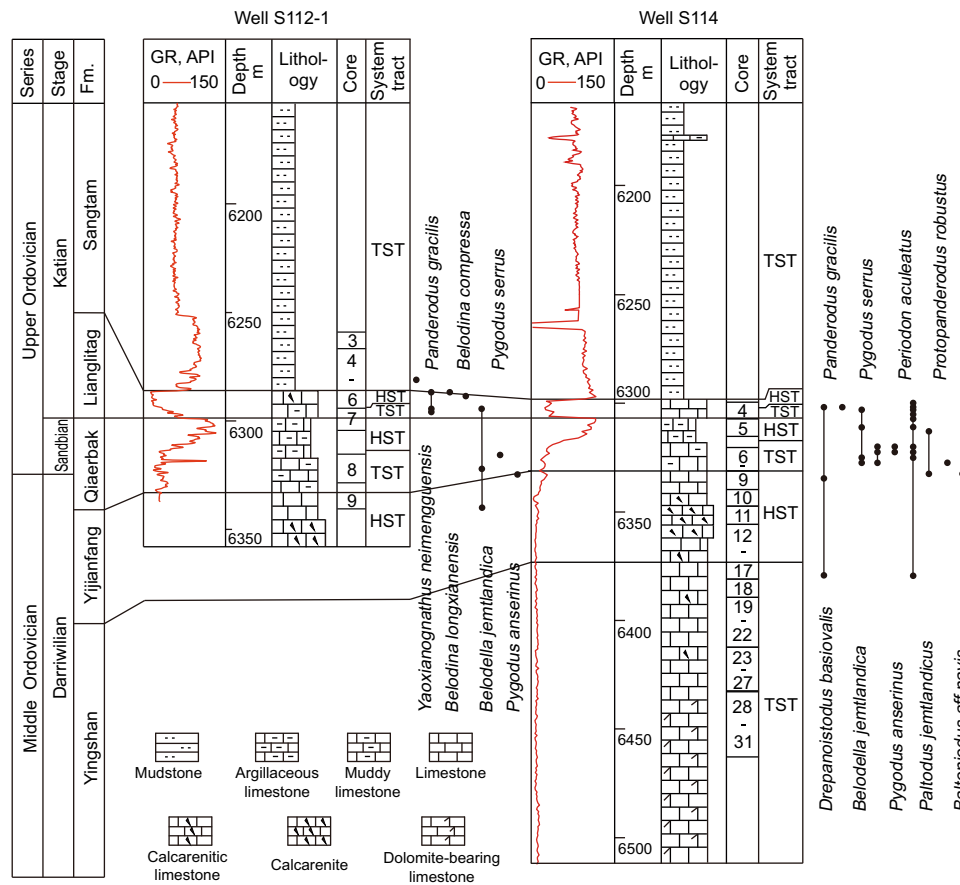


Fig. 2 Stratigraphic correlation and conodonts distribution in well S112-1 and well S114 in the Tahe oil–gas field

southwestern region was successive deposition (Liu et al. 2010). The exposed area of the Lianglitag Formation was located in the northern ramp edge. The southern region was successive deposition.

The Akekule Uplift was controlled by NW–SE extension stress in the Early Hercynian tectonic movement, so a large nose uplift plunging to the southwest was formed. The Ordovician carbonate strata were severely denuded in the northern region of the Akekule Uplift (Liu et al. 2010). The Akekule Uplift was further transformed by the Late Hercynian and Late Himalayan tectonic movements.

3 Methodology

3.1 Samples and experiments

Conodont and carbon–oxygen isotope samples for this study were collected from cores from well S112-1 and well S114 in the southern Tahe oil–gas field (Fig. 1b). The distance between the wells is 12 km. Continuous coring was not performed in the middle of the Qiaerbak Formation but separately in 11-m intervals in well S112-1 and 5-m

intervals in well S114. The total organic carbon (TOC) analysis of well S112-1 samples was also carried out. Conodont and TOC samples were analyzed by the Geological Laboratory of the Northwest Oilfield Branch Company.

Samples for carbon and oxygen isotope analysis were collected from micrites avoiding organic-rich drill cores with strong diagenesis and high argillaceous content, and from conglomerates or bands with high limy content in muddy limestones and argillaceous limestones. Samples from well S114 were collected in 2006. $\delta^{13}\text{C}_{\text{carb}}$ and $\delta^{18}\text{O}_{\text{carb}}$ analysis were measured with an MAT251 mass spectrograph in the Isotope Laboratory of Ministry of Land and Resources. Samples from well S112-1 were collected in 2010. $\delta^{13}\text{C}_{\text{carb}}$ and $\delta^{18}\text{O}_{\text{carb}}$ analysis were measured with an MAT253 mass spectrograph in the Analysis and Test Research Center of the Beijing Research Institute of Uranium Geology. The phosphate-continuous flow test method was adopted with errors less than ± 0.1 ‰ Vienna Pee Dee Belemnite (VPDB) for $\delta^{13}\text{C}_{\text{carb}}$ and less than ± 0.2 ‰ (VPDB) for $\delta^{18}\text{O}_{\text{carb}}$. The analytical process followed Liu et al. (2013). Analytical data are shown in Table 1 while the depth of samples were adjusted.

Table 1 Data of carbon and oxygen isotope for well S112-1 and well S114 (relative to VPDB standard)

Well	Formation	Depth, m	Core number	Lithology	$\delta^{13}\text{C}$, ‰	$\delta^{18}\text{O}$, ‰
S112-1	Sangtamu	6259.05	3 4/60	Mudstone	0.8	−6.1
		6262.17	3 21/60	Mudstone	0.9	−6.1
		6263.28	3 33/60	Mudstone	1.0	−5.9
		6264.52	3 39/60	Mudstone	1.0	−6.2
		6265.41	3 47/60	Mudstone	0.9	−5.9
		6266.51	3 57/60	Mudstone	0.9	−6.3
		6266.81	4 2/72	Mudstone	1.0	−6.0
		6269.93	4 18/72	Mudstone	1.0	−5.9
		6270.32	4 22/72	Mudstone	1.0	−6.1
		6271.73	4 34/72	Mudstone	1.0	−5.6
		6273.2	4 39/72	Mudstone	0.9	−6.3
		6273.4	4 42/72	Mudstone	0.9	−6.2
		6276.06	4 56/72	Mudstone	1.0	−6.3
		6276.26	4 59/72	Mudstone	0.9	−6.3
		6278.27	4 67/72	Mudstone	0.9	−6.2
		6280.27	5 3/8	Mudstone	1.0	−5.9
		6281.0	5 6/8	Mudstone	0.8	−6.5
		6281.7	6 7/106	Mudstone	0.6	−6.2
		6283.09	6 14/106	Mudstone	0.6	−6.5
		6284.49	6 27/106	Mudstone	0.9	−6.2
	6285.49	6 37/106	Mudstone	1.1	−6.1	
	Lianglitag	6286.6	6 46/106	Limestone	0.4	−5.5
		6287.57	6 53/106	Limestone	0.7	−4.8
		6288.52	6 61/106	Limestone	0.9	−5.1
		6289.7	6 70/106	Limestone	0.9	−4.5
		6290.48	6 78/106	Limestone	1.8	−3.9
		6290.97	6 87/106	Limestone	1.7	−4.2
		6291.93	6 93/106	Limestone	1.5	−4.5
		6293.04	6 103/106	Muddy limestone	1.6	−5.0
		6294.28	7 3/57	Muddy limestone	2.0	−3.9
		6295.41	7 11/57	Muddy limestone	2.5	−4.3
		6295.84	7 14/57	Muddy limestone	2.0	−4.8
		6297.11	7 24/57	Muddy limestone	2.5	−3.8
		Qiaerbak	6298.95	7 36/57	Argillaceous limestone	1.9
	6300.77		7 40/57	Argillaceous limestone	1.8	−4.5
	6300.97		7 43/57	Argillaceous limestone	1.8	−4.0
	6301.37		7 48/57	Argillaceous limestone	1.6	−4.8
	6303.77		7 56/57	Argillaceous limestone	1.0	−5.8
	6315.57		8 6/80	Muddy limestone	1.3	−4.8
	6317.45		8 11/80	Muddy limestone	1.1	−5.7
	6317.85		8 13/80	Muddy limestone	1.2	−4.4
	6319.47		8 20/80	Muddy limestone	0.9	−4.4

Table 1 continued

Well	Formation	Depth, m	Core number	Lithology	$\delta^{13}\text{C}$, ‰	$\delta^{18}\text{O}$, ‰	
S112-1	Qiaerbak	6319.93	8 27/80	Muddy limestone	1.0	−4.6	
		6320.12	8 40/80	Muddy limestone	1.3	−6.5	
		6320.75	8 43/80	Muddy limestone	1.5	−4.4	
		6322.62	8 45/80	Muddy limestone	0.9	−6.1	
		6323.42	8 51/80	Muddy limestone	0.8	−5.6	
		6324.69	8 59/80	Muddy limestone	1.0	−5.4	
		6326.21	8 67/80	Muddy limestone	0.8	−6.0	
		6327.28	8 73/80	Muddy limestone	0.5	−6.5	
		6328.5	8 80/80	Muddy limestone	0.6	−5.5	
		6329.1	9 6/47	Muddy limestone	0.6	−5.9	
		6330.71	9 12/47	Muddy limestone	0.4	−6.9	
		6331.39	9 16/47	Muddy limestone	0.4	−6.0	
		6331.64	9 19/47	Muddy limestone	0.4	−6.2	
		Yijianfang	6334.28	9 34/47	Limestone	0.5	−5.6
			6334.78	9 38/47	Limestone	0.2	−6.0
			6339.9	9 41/47	Limestone	0.3	−6.0
6340.1	9 43/47		Limestone	0.1	−6.4		
S114	Qiaerbak	6320.35	6 1/35	Muddy limestone	1.4	−4.0	
		6325.0	7 14/64	Muddy limestone	1.8	−4.7	
		6329.0	7 47/64	Muddy limestone	0.8	−5.3	
	Yijianfang	6331.2	8 13/47	Limestone	1.4	−2.6	
		6337.35	8 44/47	Limestone	0.6	−5.4	
		6339.9	10 3/69	Limestone	0.8	−5.8	
		6346.25	10 61/69	Limestone	1.2	−6.4	
		6349.55	11 21/80	Limestone	1.4	−6.5	
		6354.6	11 72/80	Limestone	0.9	−6.0	
		6358.9	12 29/39	Limestone	0.8	−6.2	
		6365.8	13 34/51	Limestone	0.6	−6.5	
		6369.86	14 26/57	Limestone	0.4	−6.2	
		6374.7	15 16/25	Limestone	0.2	−6.7	
		Yingshan	6385.1	18 37/69	Limestone	−0.2	−6.6
			6391.15	19 20/23	Limestone	−0.2	−6.5
			6397.1	20 52/73	Limestone	−0.4	−6.5
			6403.5	21 42/57	Limestone	−0.3	−6.4
			6414.85	23 14/52	Limestone	−0.3	−6.3
			6419.9	24 13/15	Limestone	−0.4	−6.5
6424.6	26 8/43		Limestone	−0.4	−6.8		
6433.15	28 4/72		Limestone	−0.6	−6.2		
6437.9	28 44/72		Limestone	−0.7	−6.0		
6442.4	29 13/75		Limestone	−0.8	−6.5		
6446.5	29 50/75	Limestone	−0.5	−6.3			
6462.8	31 64/65	Limestone	−0.8	−5.7			

3.2 Analysis of diagenetic alteration

Atmospheric freshwater diagenesis had great impacts on $\delta^{13}\text{C}_{\text{carb}}$ and $\delta^{18}\text{O}_{\text{carb}}$ ratios of carbonate rocks leading to

the values of $\delta^{13}\text{C}_{\text{carb}}$ and $\delta^{18}\text{O}_{\text{carb}}$ decreasing significantly (Gradstein et al. 2012). The top surface of the Yijianfang and Lianglitag Formations in the Tahe oil–gas field had been exposed for a short time and undergone atmospheric

freshwater karstification. The exposed areas are located, respectively, in the northeastern and northern regions of the study area. Well S112-1 and well S114 exhibited successive deposition in the Middle–Upper Ordovician, indicating the samples from these wells were unlikely to have been altered by atmospheric freshwater. The $\delta^{13}\text{C}_{\text{carb}}$ and $\delta^{18}\text{O}_{\text{carb}}$ curves in the upper Yijianfang Formation of well S112-1 showed positive excursion features (Fig. 3). Discordant phenomena appeared in the upper Yijianfang Formation of well S114. These characteristics reflected that the samples were less affected by meteoric water.

Compared with $\delta^{13}\text{C}_{\text{carb}}$, $\delta^{18}\text{O}_{\text{carb}}$ is more susceptible to the influence of diagenesis (Gradstein et al. 2012; Metzger et al. 2014). The initial composition of $\delta^{13}\text{C}_{\text{carb}}$ may be obviously changed when the $\delta^{18}\text{O}_{\text{carb}}$ value is less than -10‰ (Derry et al. 1992). The $\delta^{18}\text{O}_{\text{carb}}$ values of well S112-1 and well S114 were both more than -10‰ , reflecting that the $\delta^{13}\text{C}_{\text{carb}}$ value of samples from the two wells has been influenced by relatively weak diagenesis.

Correlation of $\delta^{13}\text{C}_{\text{carb}}$ and $\delta^{18}\text{O}_{\text{carb}}$ is also a method for judging diagenetic alteration of carbonate rock samples (Sial et al. 2013). It is indicated that the $\delta^{13}\text{C}_{\text{carb}}$ and $\delta^{18}\text{O}_{\text{carb}}$ of partial samples had an obvious positive association (Fig. 4), which appeared in the upper Yijianfang Formation to middle Qiaerbak Formation, upper Qiaerbak Formation to lower Lianglitag Formation, and middle–upper

Lianglitag Formation (Fig. 3). But these positive associations had no relationship with depth, but with formations (as shown in Fig. 3). The correlation of $\delta^{13}\text{C}_{\text{carb}}$ and $\delta^{18}\text{O}_{\text{carb}}$ from the Yingshan Formation to the lower Yijianfang Formation in well S114 was not good because of weak fluctuations. The coordination change phenomenon of $\delta^{13}\text{C}_{\text{carb}}$ and $\delta^{18}\text{O}_{\text{carb}}$ in Middle–Late Ordovician also occurred in South America (Sial et al. 2013). Therefore, this positive association might reflect a coordination change relationship between $\delta^{13}\text{C}_{\text{carb}}$ and $\delta^{18}\text{O}_{\text{carb}}$ in a specific sedimentary background, indicating a fluctuation trend of $\delta^{13}\text{C}_{\text{carb}}$ and $\delta^{18}\text{O}_{\text{carb}}$ of original seawater.

4 Results

4.1 Carbon isotope curve of well S114

The $\delta^{13}\text{C}_{\text{carb}}$ curve from the Yingshan Formation to the Qiaerbak Formation in well S114 showed generally positive excursion features (Fig. 3), ranging from -0.8 to 1.8‰ . The excursion process could be divided into three intervals, where intervals A and C were positive excursions. The fluctuation range of interval A is the largest, about 2.2‰ among the three intervals with a maximum $\delta^{13}\text{C}_{\text{carb}}$ value of 1.4‰ . Interval B appeared in the upper

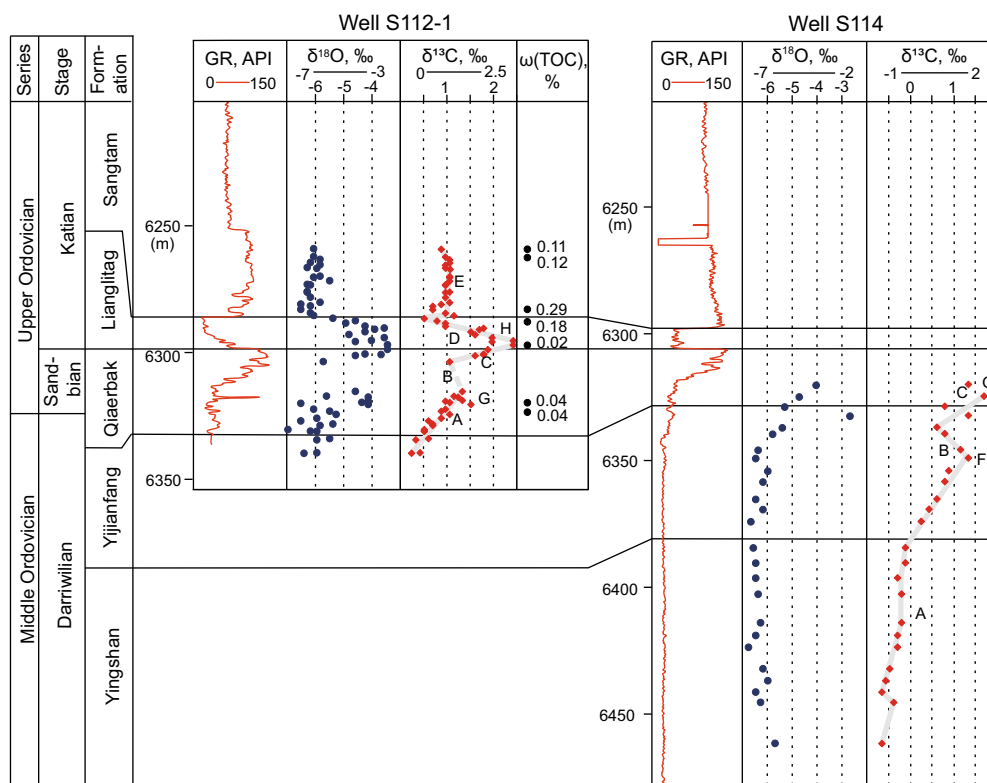


Fig. 3 The curves of $\delta^{13}\text{C}_{\text{carb}}$ and $\delta^{18}\text{O}_{\text{carb}}$ in the Middle–Upper Ordovician for well S112-1 and well S114 in the Tahe oil–gas field

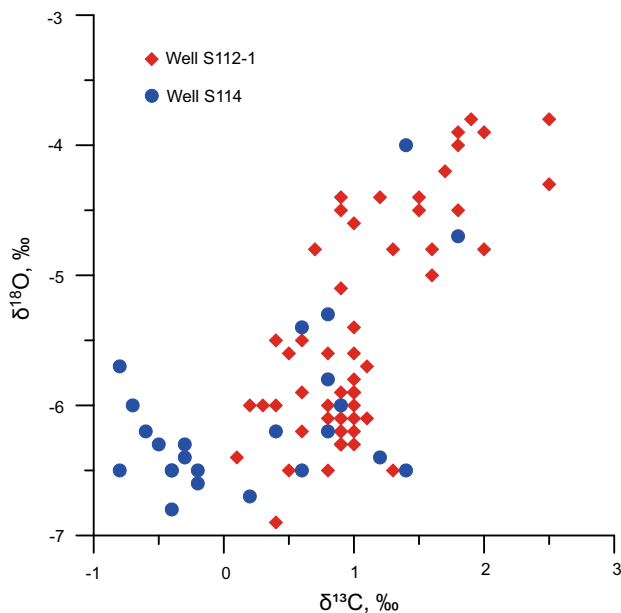


Fig. 4 Cross plot of $\delta^{13}\text{C}_{\text{carb}}$ versus $\delta^{18}\text{O}_{\text{carb}}$ for well S112-1 and well S114 in the Tahe oil-gas field

part of the Yijianfang Formation with the $\delta^{13}\text{C}_{\text{carb}}$ value moving -0.8‰ compared with the value below. Interval C appeared from the top part of the Yijianfang Formation to the lower part of the Qiaerbak Formation with the fluctuation range reaching 1.2‰ .

4.2 Carbon isotope curve of Well S112-1

The $\delta^{13}\text{C}_{\text{carb}}$ curve of well S112-1 fluctuates sharply from a minimum value of 0.1‰ at the top of the Yijianfang Formation to a peak value of 2.5‰ in the Lianglitag Formation. The excursion process in this well can be divided into five intervals. Interval A is a positive excursion, where the $\delta^{13}\text{C}_{\text{carb}}$ values shift from 0.1 to 1.3‰ from the top of the Yijianfang Formation to the lower Qiaerbak Formation. Interval B is a negative excursion, where the fluctuation range of $\delta^{13}\text{C}_{\text{carb}}$ values in the middle of the Qiaerbak Formation is at least -0.3‰ . This negative excursion is estimated from the difference between upper and lower values, because of non-coring in this well. But it is confirmed by other wells drilled in the western Tabei Uplift (Bao et al. 2006). Interval C is a positive excursion, and the $\delta^{13}\text{C}_{\text{carb}}$ values fluctuate up to 1.4‰ from the top of the Qiaerbak Formation to the bottom of the Lianglitag Formation. Interval D is a negative excursion, where $\delta^{13}\text{C}_{\text{carb}}$ values decrease rapidly in the upper part of the Lianglitag Formation and fluctuate up to 2.1‰ . Interval E appears in the lower Sangtamu Formation, where the $\delta^{13}\text{C}_{\text{carb}}$ values with positive excursion quickly move to near 1‰ and narrowly fluctuate around 1‰ .

From the characteristics of $\delta^{13}\text{C}_{\text{carb}}$ curves in Fig. 3, there are mainly three $\delta^{13}\text{C}_{\text{carb}}$ -positive excursions from F

to H occurring in well S114 and well S112-1, developing in the Yijianfang Formation, Upper Yijianfang Formation to lower Qiaerbak Formation, and upper Qiaerbak Formation to the middle Lianglitag Formation, respectively.

5 Discussion

Well S112-1 and well S114 are relatively close to each other and their sedimentary environment is also similar. Therefore, taking the top of the Yijianfang Formation as the boundary, $\delta^{13}\text{C}_{\text{carb}}$, $\delta^{18}\text{O}_{\text{carb}}$, and logging curves of the two wells were put together to contrast with the Ordovician $\delta^{13}\text{C}_{\text{carb}}$ curve of the Kalpin outcrop (Hu et al. 2010) and the generalized curve of the world (Albanesi et al. 2013) (Figs. 5, 6).

5.1 Positive carbon isotope excursions and sea level change

A $\delta^{13}\text{C}_{\text{carb}}$ excursion in a stratigraphic succession may simply record the lateral movement of an isotopically unique water body during a sea level change. Considering the asynchronization of sea level change, $\delta^{13}\text{C}_{\text{carb}}$ excursions resulting from sea level change have few contributions to global comparison (Edwards and Saltzman 2014). Therefore, the relationship between three $\delta^{13}\text{C}_{\text{carb}}$ -positive excursions shown in Figs. 3 and 5 with sea level changes is very important.

According to research on Ordovician sequence stratigraphy in the Tahe oil-gas field and Tarim Basin and our results shown in Fig. 2 (Deng et al. 2007; Wu et al. 2012; Liu et al. 2012), the positive excursion A occurred in the HST of the Yijianfang Formation, the positive excursion B in the TST of the Qiaerbak Formation, and the positive excursion C in the HST of the Qiaerbak Formation and the TST of the Lianglitag Formation, which indicated that three positive excursions had no direct relationships with sea level fluctuation, and could be correlated regionally or globally.

5.2 Correlation of $\delta^{13}\text{C}_{\text{carb}}$ -positive excursions in the Tarim Basin and the world

The *Pygodus serra* conodont zone in the Darriwilian, the *P. anserinus* conodont zone in the Sandbian, and the *Belodina compressa* conodont zone in the Early Katian (shown in Fig. 2) of the Tahe oil-gas field in the northern Tarim Basin can be compared or partly compared with that of the Argentine Precordillera (Sial et al. 2013; Albanesi et al. 2013; Edwards and Saltzman 2014), Oklahoma and Virginia, USA (Young et al. 2008), Cincinnati region, USA (Bergström et al. 2010), Sweden (Wu et al. 2015), and

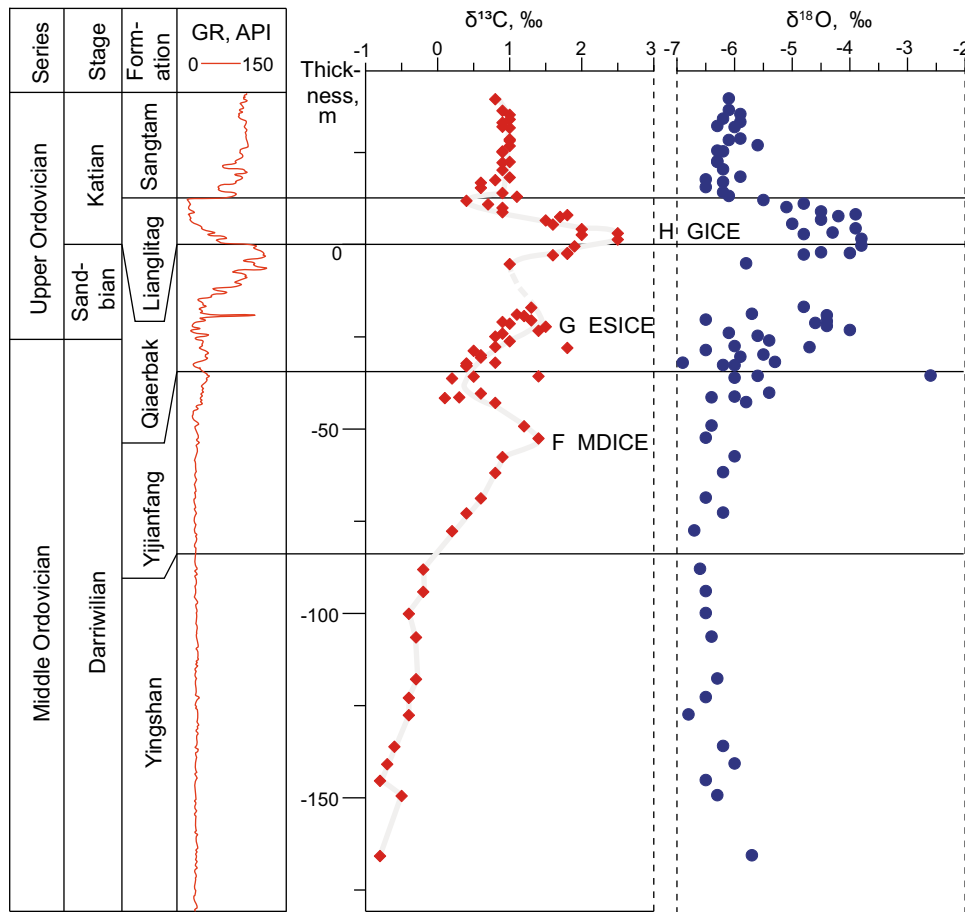


Fig. 5 The curves of $\delta^{13}\text{C}_{\text{carb}}$ and $\delta^{18}\text{O}_{\text{carb}}$ of the Dariwilian–Early Katian in the Tahe oil–gas field

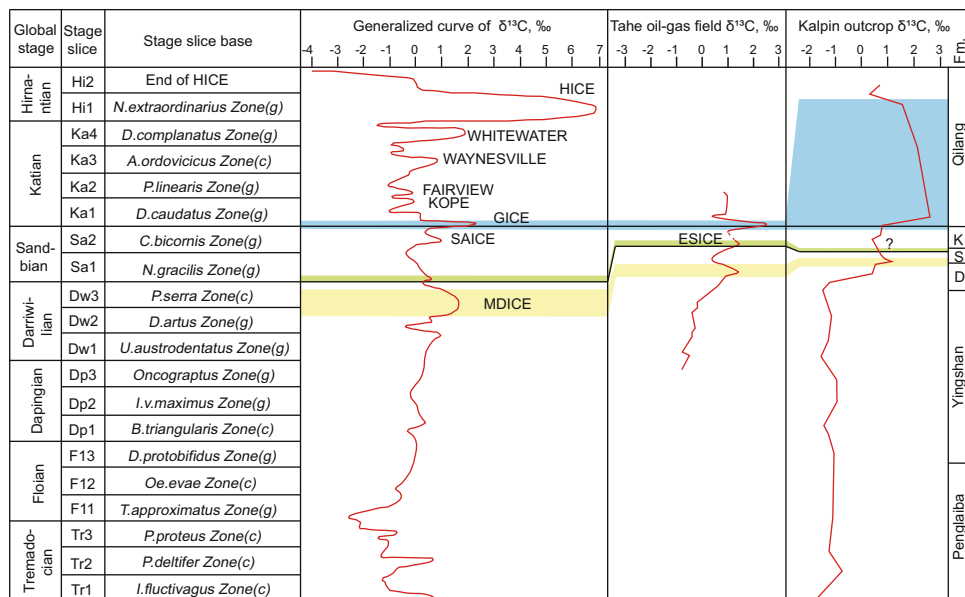


Fig. 6 The $\delta^{13}\text{C}_{\text{carb}}$ curve of the Dariwilian–Early Katian in the Tahe oil–gas field contrasting with the Ordovician $\delta^{13}\text{C}_{\text{carb}}$ curves of the Kalpin outcrop and the world. *g* graptolite zonation, *c* conodont

zonation, *D* Dawangou Formation, *S* Saergan Formation, and *K* Kanling Formation

Baltoscandia (Ainsaar et al. 2010), which provides a basis for time limits on $\delta^{13}\text{C}_{\text{carb}}$ -positive excursions.

According to Figs. 5 and 6, the positive excursion F in the Middle Ordovician Yijianfang Formation corresponds with the MDICE of the global Ordovician $\delta^{13}\text{C}$ curve, with a peak value generally less than 2 ‰ in South China, North America, South America, and Europe. Positive excursion H is consistent with the GICE. Maximum $\delta^{13}\text{C}_{\text{carb}}$ values are generally less than 3 ‰. However, it is slightly greater than 3 ‰ in Pennsylvania (Pancost et al. 2013) and Virginia (Young et al. 2008), USA. Evidence of the GICE from the upper Sandbian can also be found in Oklahoma, USA (Rosenau et al. 2012).

Positive excursion G between the MDICE and GICE in the Tahe oil–gas field was developed in *P. anserinus* conodont zone of the Early Sandbian. The fluctuation range was more than the corresponding positive excursion in the global Ordovician curve (Fig. 6). This excursion is currently not officially named, so in this paper, it is named the ESICE. Sandbian carbon isotope excursion (SAICE), also called the Spechts Ferry Excursion, in the Late Sandbian close to the GICE was not found in the Tahe oilfield (Fig. 6). Whether it can be globally correlated or not is controversial (Sial et al. 2013).

Chen et al. (2012) argues the age of the Middle–Upper Ordovician Saergan Formation black shale in the Kalpin outcrop is from the Middle Darriwilian to the Early Sandbian from graptolite data. According to Fig. 6, the MDICE of the Yijianfang Formation in the Tahe oil–gas field is equivalent to the positive excursion in the bottom of the Saergan Formation. But the features of the ESICE in the Saergan Formation are not clear, which might be caused by sparse sampling points. The positive excursion of the Qilang Formation corresponded with the GICE. The Lianglitag Formation positive excursions from drill cores and cuttings in the Bachu and Tazhong Uplifts were in accordance with the GICE in the Tahe oil–gas field (Zhang et al. 2014). Because of the absence of the Darriwilian–Sandbian in the Bachu and Tazhong Uplifts, the ESICE and MDICE might be developed in areas with consecutive strata.

5.3 Genesis of positive carbon isotope excursion

According to outcrop and drilling data from the Tarim Basin, Ordovician source rocks consist of the Middle–Lower Ordovician Heituwa Formation in the Manjiaer Depression (Fig. 1a), the Middle–Upper Ordovician Saergan Formation in the Kalpin outcrop and the Upper Ordovician Lianglitag Formation in the basin (Wang 2000; Zhang et al. 2006; Gao et al. 2007; Zhao et al. 2008). The thickness of the Heituwa Formation source rock can reach a maximum of 56 m with an average TOC of 3.1 % (Zhao

et al. 2008). There are no published carbon isotope data from cores in the Heituwa Formation. Chen et al. (2012) believed the age of the Heituwa Formation in the Kuruktag outcrop should be Middle Tremadocian—Early Darriwilian. The genesis of this source rock may be related to the increase in organic matter productivity and organic carbon burial which was caused by a gradual decline in sea surface temperature during the Early to Middle Ordovician (Trotter et al. 2008).

The thickness of the Saergan Formation source rocks in the Kapin outcrop is 13.8 m with an average TOC of black shale of 1.92 % (Gu et al. 2012). The age of the Saergan Formation corresponds with the MDICE and ESICE (shown in Fig. 6). The Upper Ordovician Lianglitag Formation source rocks had been characterized by drilling in the Tazhong and Tabei Uplifts (Gao et al. 2007; Zhao et al. 2008), with an average TOC of 1.1 % and 0.5 %, respectively (Zhao et al. 2008). The age of Lianglitag Formation source rocks corresponds with the GICE. The Shuntuo-guole low uplift and Awati fault depression, between the Tabei and Tazhong Uplifts, were located in a low area during the deposition of the Lianglitag Formation, and may be favorable for source rock development corresponding with the GICE (Fig. 1a).

Carbon isotope reversal in kerogen and soluble organic components of Cambrian and Ordovician carbonate rocks in the Tarim Basin is common, which may be controlled by thermal evolution or parent materials (Zhang et al. 2006; Liu et al. 2013a). Enrichment of ^{13}C in residues of kerogen during thermal evolution can make the $\delta^{13}\text{C}$ of source rock heavier. The TOC value of the Qiaerbak to Sangtamu Formations in the Upper Ordovician of well S112-1 is low (Fig. 3), which indicates that the source rock is not developed. Therefore, the genesis of the MDICE, ESICE, and GICE was not related to the kerogen thermal evolution, but to the $\delta^{13}\text{C}_{\text{carb}}$ value increase in carbonate rocks by massive amounts of organic matter buried during the deposition period.

6 Conclusions

- (1) There are three $\delta^{13}\text{C}_{\text{carb}}$ -positive excursions identified in the Middle–Upper Ordovician (Darriwilian—Early Katian) in the Tahe oil–gas field according to the conodont biostratigraphy. The positive excursions have no direct relation with sea level fluctuations. The MDICE and GICE could be globally correlated.
- (2) The $\delta^{13}\text{C}_{\text{carb}}$ -positive excursion within the *P. anserinus* conodont zone developed in the Early Sandbian was named the ESICE in this paper. The fluctuation range of the ESICE is less than that of the MDICE

and GICE. Previous studies have paid little attention on this excursion. Whether the ESICE can be applied to global correlation or not needs further investigation.

- (3) The genesis of the Saergan Formation marine source rocks of the Middle–Upper Ordovician in the Kalpin outcrop was in accord with the MDICE and ESICE. But the GICE had strong ties to the source rock of the Lianglitag Formation in the basin. These relationships indicated that massive organic carbon burial is an important factor controlling the genesis of the $\delta^{13}\text{C}_{\text{carb}}$ -positive excursion.

Acknowledgments The authors are grateful to three anonymous reviewers for their constructive reviews. This work was supported by the National Key Scientific Project of China (No. 2011ZX05005-004; 2016ZX05005-002) and the National Basic Research Program of China (973 Program) (No. 2012CB214806).

Open Access This article is distributed under the terms of the Creative Commons Attribution 4.0 International License (<http://creativecommons.org/licenses/by/4.0/>), which permits unrestricted use, distribution, and reproduction in any medium, provided you give appropriate credit to the original author(s) and the source, provide a link to the Creative Commons license, and indicate if changes were made.

References

- Ainsaar L, Kaljo D, Martma T, et al. Middle and Upper Ordovician carbon isotope chemostratigraphy in Baltoscandia: a correlation standard and clues to environmental history. *Palaeogeog Palaeoclimatol Palaeoecol.* 2010;294(3–4):189–201.
- Albanesi GL, Bergström SM, Schmitz B, et al. Darrivilian (Middle Ordovician) $\delta^{13}\text{C}_{\text{carb}}$ chemostratigraphy in the Precordillera of Argentina: documentation of the Middle Darrivilian isotope carbon excursion (MDICE) and its use for intercontinental correlation. *Palaeogeog Palaeoclimatol Palaeoecol.* 2013;389(4):48–63.
- Bao ZD, Jin ZJ, Sun LD, et al. Sea-level fluctuation of the Tarim area in the Early Paleozoic responded from geochemistry and karst. *Acta Geol Sin.* 2006;80(3):366–73 (in Chinese).
- Bergström SM, Young S, Schmitz B. Katian (Upper Ordovician) $\delta^{13}\text{C}$ chemostratigraphy and sequence stratigraphy in the United States and Baltoscandia: a regional comparison. *Palaeogeog Palaeoclimatol Palaeoecol.* 2010;296(3–4):217–34.
- Chen X, Bergström SM, Zhang YD, et al. A regional tectonic event of Katian (Late Ordovician) age across three major blocks of China. *Chin Sci Bull.* 2013;58(34):4292–9.
- Chen X, Wang ZH. Global auxiliary stratotype section of the Upper Ordovician in China. *J Stratig.* 2003;27(3):264–6 (in Chinese).
- Chen X, Zhang YD, Li Y, et al. Biostratigraphic correlation of the Ordovician black shales in Tarim Basin and its peripheral regions. *Chin Sci Bull.* 2012;55(8):1230–7.
- Deng XJ, Li GR, Xu GS, et al. Sequence stratigraphic study, prediction and quality evaluation of reservoir for the Ordovician Yijianfang Formation of the Southern part of Tahe Oilfield. *Acta Sedimentol Sin.* 2007;25(3):392–400 (in Chinese).
- Derry LA, Kaufman AJ, Jacobsen SB. Sedimentary cycling and environmental change in the Late Proterozoic: evidence from stable and radiogenic isotopes. *Geochim Cosmochim Acta.* 1992;56(3):1317–29.
- Edwards CT, Saltzman MR. Carbon isotope ($\delta^{13}\text{C}_{\text{carb}}$) stratigraphy of the Lower–Middle Ordovician (Tremadocian–Darrivilian) in the Great Basin, Western United States: implications for global correlation. *Palaeogeog Palaeoclimatol Palaeoecol.* 2014;399:1–20.
- Fan R, Deng SH, Zhang XL. Significant carbon isotope excursions in the Cambrian and their implications for global correlations. *Sci China Earth Sci.* 2011;54(11):1686–95.
- Gao ZY, Zhang SC, Zhang XY, et al. Relations between spatial distribution and sequence types of the Cambrian–Ordovician marine source rocks in Tarim Basin. *Chin Sci Bull.* 2007;52(S1):92–102.
- Gradstein FM, Ogg JG, Schmitz MD, et al. The geologic time scale. London: Elsevier Science Ltd; 2012.
- Gu Y, Zhao YQ, Jia CS, et al. Analysis of hydrocarbon resource potential in Awati Depression of Tarim Basin. *Pet Geol Exp.* 2012;34(3):257–66 (in Chinese).
- Hu MY, Qian Y, Hu ZG, et al. Carbon isotopic and element geochemical responses of carbonate rocks and Ordovician sequence stratigraphy in Keping area. Tarim Basin. *Acta Pet Mineral.* 2010;29(2):199–205 (in Chinese).
- Jing XC, Deng SH, Zhao ZJ, et al. Carbon isotope composition and correlation across the Cambrian–Ordovician boundary in Keping region of the Tarim Basin. China. *Sci China Earth Sci.* 2008;51(9):1317–29.
- Liu CG, Li T, Lv HT, et al. Stratigraphic division of Middle–Upper Ordovician and characteristics of the first episode karstification of Middle Caledonian in Akekule uplift, Xinjiang, China. *J Chengdu Univ Technol Sci Technol Ed.* 2010;37(1):55–63 (in Chinese).
- Liu H, Liao ZW, Zhang HZ, et al. Review of the study on stable carbon isotope reversal between kerogen and its evolution products: implication for the research of the marine oil reservoirs in the Tarim Basin, NW China. *Bull Mineral Pet Geochem.* 2013a;32(4):497–502 (in Chinese).
- Liu HB, Jin GS, Li JJ, et al. Determination of stable isotope composition in uranium geological samples. *World Nucl Geosci.* 2013b;30(3):174–9 (in Chinese).
- Liu JQ, Li Z, Huang JC, et al. Distinct sedimentary environments and their influences on carbonate reservoir evolution of the Lianglitag Formation in the Tarim Basin, Northwest China. *Sci China Earth Sci.* 2012;55(10):1641–55.
- Metzger JG, Fike DA, Smith LB. Applying carbon-isotope stratigraphy using well cuttings for high-resolution chemostratigraphic correlation of the subsurface. *AAPG Bull.* 2014;98(8):1551–76.
- Munnecke A, Calner M, Harper DAT, et al. Ordovician and Silurian sea-water chemistry, sea level, and climate: a synopsis. *Palaeogeog Palaeoclimatol Palaeoecol.* 2010;296(3–4):389–413.
- Munnecke A, Zhang YD, Liu X, et al. Stable carbon isotope stratigraphy in the Ordovician of South China. *Palaeogeog Palaeoclimatol Palaeoecol.* 2011;307(1–4):17–43.
- Pancost RD, Freeman KH, Herrmann AD, et al. Reconstructing Late Ordovician carbon cycle variations. *Geochim Cosmochim Acta.* 2013;105:433–54.
- Rosenau NA, Herrmann AD, Leslie SA. Conodont apatite $\delta^{18}\text{O}$ values from a platform margin setting, Oklahoma, USA: implications for initiation of Late Ordovician icehouse conditions. *Palaeogeog Palaeoclimatol Palaeoecol.* 2012;315–316:172–80.
- Saltzman MR. Phosphorus, nitrogen, and the redox evolution of the Paleozoic oceans. *Geology.* 2005;33(7):573–6.
- Sial AN, Peralta S, Gaucher C, et al. High-resolution stable isotope stratigraphy of the Upper Cambrian and Ordovician in the Argentine Precordillera: carbon isotope excursions and correlations. *Gondwana Res.* 2013;24(1):330–48.

- Thompson CK, Kah LC. Sulfur isotope evidence for widespread euxinia and a fluctuating oxycline in Early to Middle Ordovician greenhouse oceans. *Palaeogeog Palaeoclimatol Palaeoecol.* 2012;313–314:189–214.
- Torsvik TH, Cocks LRM. Gondwana from top to base in space and time. *Gondwana Res.* 2013;24(3–4):999–1030.
- Trotter JA, Williams IS, Barnes CR, et al. Did cooling oceans trigger Ordovician biodiversification? *Evid Conodont Thermom Sci.* 2008;321(5888):550–4.
- Wang DR. Macro-evidence of carbonate isotopes for the Middle–Upper Ordovician source rocks in the Tarim Basin. *Geol Rev.* 2000;46(3):328–34 (in Chinese).
- Wang HH, Li JH, Yang JY, et al. Paleo-plate reconstruction and drift path of Tarim Block from Neoproterozoic to Early Palaeozoic. *Adv Earth Sci.* 2013a;28(6):637–47 (in Chinese).
- Wang XL, Hu WX, Li Q, et al. Negative carbon isotope excursion on the Cambrian series 2–series 3 boundary for Penglaiba section in Tarim Basin and its significances. *Geol Rev.* 2011;57(1):16–23 (in Chinese).
- Wang ZH, Qi YP, Bergström SM. Ordovician conodonts of the Tarim region, Xinjiang, China: occurrence and use as palaeoenvironment indicators. *J Asian Earth Sci.* 2007;29(5–6):832–43.
- Wang ZH, Wu RC, Bergström SM. Ordovician conodonts from the Lunnan area of Northwestern Taklimakan desert, Xinjiang, China, with remarks on the evolution of pygodus. *Acta Palaeontol Sin.* 2013b;54(2):408–23 (in Chinese).
- Wang ZZ, Yang JD. Features of the carbon isotope changes in the Early Palaeozoic rocks of the Kalpin area, Xinjiang and their significance. *J Stratig.* 1994;18(1):45–52 (in Chinese).
- Wu RC, Calner M, Lehnert O, et al. Lower–Middle Ordovician 13C chemostratigraphy of western Baltica (Jämtland, Sweden). *Palaeoworld.* 2015;24(1–2):110–22.
- Wu XN, Shou JF, Zhang HL, et al. Characteristics of the petroleum system in Cambrian and Ordovician sequence frameworks of the Tarim Basin and its exploration significance. *Acta Pet Sin.* 2012;33(2):225–31 (in Chinese).
- Young SA, Saltzman MR, Bergström SM, et al. Paired $\delta^{13}\text{C}_{\text{carb}}$ and $\delta^{13}\text{C}_{\text{org}}$ records of Upper Ordovician (Sandbian–Katian) carbonates in North America and China: implications for paleoceanographic change. *Palaeogeog Palaeoclimatol Palaeoecol.* 2008;270(1–2):166–78.
- Zhang YD, Cheng JF, Munnecke A, et al. Carbon isotope development in the Ordovician of the Yangtze Gorges region (South China) and its implication for stratigraphic correlation and paleoenvironmental change. *J Earth Sci.* 2010a;21(S1):70–4.
- Zhang YD, Zhan RB, Fan JX, et al. Principal aspects of the Ordovician biotic radiation. *Sci China Earth Sci.* 2010b;53(3):282–394.
- Zhang ZL, Li HL, Tan GH, et al. Carbon isotope chemostratigraphy of the Ordovician system in Central Uplift of the Tarim Basin. *J Stratig.* 2014;38(2):181–9 (in Chinese).
- Zhang ZN, Liu WH, Zheng JJ, et al. Carbon isotopic reversed distribution of the soluble organic components for the Cambrian and Ordovician carbonate rocks in Tabei and Tazhong areas, Tarim Basin. *J Mineral Pet.* 2006;26(4):69–74 (in Chinese).
- Zhao MJ, Wang ZM, Pan WQ, et al. Lower Palaeozoic source rocks in Manjiaer Sag, Tarim Basin. *Pet Explor Dev.* 2008;34(4):417–23 (in Chinese).
- Zhao ZJ. Indicators of global sea-level change and research methods of marine tectonic sequences: taking Ordovician of the Tarim Basin as an example. *Acta Pet Sin.* 2015;36(3):262–73 (in Chinese).
- Zhao ZJ, Zhao ZX, Huang ZB. Ordovician conodont zones and sedimentary sequences of the Tarim Basin, Xinjiang, NW China. *J Stratig.* 2006;30(3):193–203 (in Chinese).